# Stability Lobes Prediction in Thin Wall Machining

O. B. Adetoro, P. H. Wen*, W. M. Sim, R. Vepa

*Abstract*— **A Finite Element Analysis (FEA) and Fourier transform approach to obtain frequency response function (FRF) is presented in this paper. The aim in this paper is to eliminate the need for the classical impact experimental approach used in extracting structure's FRF.**

**The numerical and experimental FRFs have been used to obtain stable regions in machining of thin walled structures, which gives a good comparison. Examples are presented and compared with experimental results with a satisfactory agreement.**

*Index Terms*— **FEA, frequency response function, discrete Fourier transform, stability lobes, transfer function.**

## I. INTRODUCTION

Even after such an extensive research into chatter vibration, it still is (as stated by Taylor just over a century ago) one of the most obscure and delicate of all problems facing the machinist [1]. It certainly undermines and reduces productivity and surface quality in manufacturing. It could also increase the cost through possible machine or tool damage. It is because of these effects that it has been the topic of several studies over the years. The stability lobes/chart approach is more practical from the stance of a machinist, while its extraction can be somewhat tedious. The accuracy of the predicted stable region relies on the transfer function identified at the cutter-workpiece contact zone. The classical approach to obtaining the transfer function is through impact test. However, this paper proposes an alternative approach which uses finite element method (FEM) modal analysis to obtain the transfer function at specified cutter-workpiece contact zones.

While the transfer functions for the tool can be assumed to be constant, the workpiece transfer function/dynamics are constantly changing as material is removed. Moreover, in thin wall machining, the workpiece vibration is significant compared to that of the tool. Hence the transfer function used must be precise. It will be highly impractical to perform impact tests at multiple stages of machining, hence the need for an offline approach to stability lobes prediction.

The prediction of stable conditions in the form of charts started when, Tobias [2] and Tlusty [3] simultaneously made the remarkable discovery that the main source of self-excited regenerative vibration/chatter was not related to the presence of negative process damping as was previously assumed. However, it is related to the structural dynamics of the machine tool-workpiece system and the feedback response between subsequent cuts. Though, a pioneering research, their model is only applicable to orthogonal metal cutting where the directional dynamic milling coefficients are constant and not periodic. Other studies on the stability of orthogonal metal cutting were reported Merritt [4].

Sridhar et al. [5] carried out an in-depth study in which, they introduced time-varying directional coefficients in their chatter stability analysis. They used the system's state transition matrix in their stability model, which helps to eliminate the periodic and time delay terms. Slavicek [6] and Vanherck [7] made the assumption that all the cutter teeth have a constant directional orientation in their study of the effect of irregular pitch on the stability. Tlusty [8] made an attempt to apply the orthogonal model to milling process by assuming the teeth of the tool had equal pitch, was simultaneously in cut and that the motion was rectilinear with constant depth of cut. Optiz et al. [9, 10] used an average value of the periodic directional coefficients in the analysis. The Nyquist criterion was used by Minis and Yanushevsky [11, 12] and Lee et al. [13, 14] to obtain the stability limits. Lee et al. used the mean value method to replace the time varying directional coefficients by a constant. Altintas and Budak [15] later proposed an analytic approach in which the average value in the Fourier series expansion (single frequency solution) of the time varying coefficients was adopted. This is the main analytical approach generally used in predicting stable cutting conditions in machining [16, 17, 18, 19]. Budak and Altintas [20, 21] later showed that the results obtained by including the harmonic terms (multi-frequency solution) are very close to the single frequency solution.

This paper presents a numerical approach to obtaining the structures transfer function, which is required in the stability model. This approach aims to eliminate the need for series of experimental impact testing at various points on a thin walled workpiece in order to obtain the transfer function.

## II. CHATTER STABILITY MODEL

The stability model used in this paper is the model

Manuscript received March 18, 2009. This work was supported in part by EPSRC and Airbus UK under Grant BS123456.

O. B. Adetoro is with Queen Mary University of London, Queen Mary, University of London, Mile End Road, London E1 4NS, UK (e-mail: o.adetoro@qmul.ac.uk).

*P. H. Wen is with Queen Mary University of London, Queen Mary, University of London, Mile End Road, London E1 4NS, UK; (phone: 44(0)20-7882-5371, fax: 44(0)20-8983-1007; email: p.h.wen@qmul.ac.uk).

W. M. Sim is with Airbus, New Filton House, Golf Course Lane, Filton BS34 7AR, UK (e-mail: WeiMing.Sim@airbus.com).

R. Vepa is with Queen Mary University of London, Queen Mary, University of London, Mile End Road, London E1 4NS, UK (e-mail: r.vepa@qmul.ac.uk).

proposed by Altintas and Budak [15] as summarized below. The periodic milling forces excite the cutter and the workpiece causing two orthogonal dynamic displacements

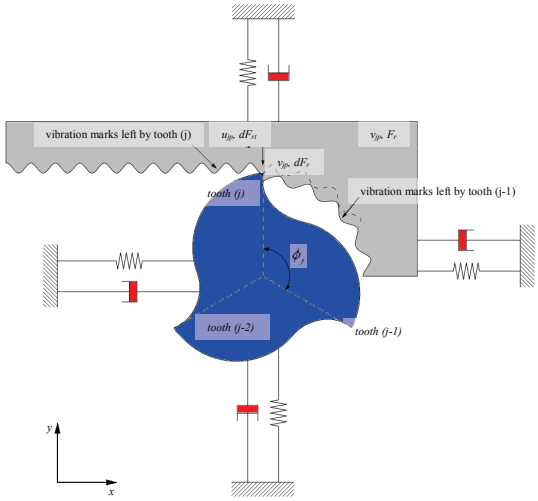


Fig. 1 – Dynamic Milling Model.

$x$ and $y$ in the global axis. This generates undulations on the machined surface and each tooth removes the undulations generated by the previous tooth (see Figure 1). Therefore leading to a modulated chip thickness which can be expressed as

$$h_j(\phi) = s_t \sin\phi_j + \left(\upsilon_{jc}^0 - \upsilon_{jw}^0\right) - \left(\upsilon_{jc} - \upsilon_{jw}\right), \quad (1)$$

where $s_t$ is the feed per tooth, $\left(\upsilon_{jc}^0, \upsilon_{jc}\right)$ and $\left(\upsilon_{jw}^0, \upsilon_{jw}\right)$ are the dynamic displacement of the cutter and workpiece at the previous and present tooth periods respectively, $\phi_j = (j-1)\phi_p + \Omega t$ is the angular immersion of tooth $j$ for a cutter ($\Omega$ if the angular speed), with constant pitch angle $\phi_p = 2\pi/N$ ($N$ is the number of teeth).

The dynamic displacements in the chip thickness direction due to tool and workpiece vibrations are defined as

$$\upsilon_{jp} = -x_p \sin\phi_j - y_p \cos\phi_j \quad (p = c, w), \quad (2)$$

where $c$ and $w$ indicate the cutter and workpiece respectively, $x_p, y_p$ and $x_p^0, y_p^0$ are the dynamic displacements in the global axis for the current and previous tooth periods respectively.

By eliminating the static part in (1), the dynamic chip thickness in milling is defined as

$$h_j(\phi) = \Delta x \sin\phi_j - \Delta y \cos\phi_j, \quad (3)$$

where,

$$\Delta x = \left(x_c - x_c^0\right) - \left(x_w - x_w^0\right),$$
$$\Delta y = \left(y_c - y_c^0\right) - \left(y_w - y_w^0\right), \quad (4)$$

Therefore, the dynamic forces on tooth $j$ (using ''Exponential Force Coefficient Model'', [22]) in the tangential and radial directions can be defined as

$$F_{tj}(\phi) = K_t a h_j(\phi),$$
$$F_{rj}(\phi) = K_r F_{tj}(\phi), \quad (5)$$

where $a$ is the axial depth of cut (ADOC), and $K_t$ and $K_r$ are the tangential and radial cutting force coefficients respectively. By substituting (3) into (5) and resolving in the global directions, the following expression is obtained

$$\begin{Bmatrix} F_x \\ F_y \end{Bmatrix} = \frac{1}{2} a K_t \begin{bmatrix} a_{xx} & a_{xy} \\ a_{yx} & a_{yy} \end{bmatrix} \begin{Bmatrix} \Delta x \\ \Delta y \end{Bmatrix}, \quad (6)$$

where $a_{xy}$ are the periodic directional cutting coefficients and depends on the angular position of the cutter and the radial cutting force coefficient $K_r$, thereby making (6) a function of time

$$\{F(t)\} = \frac{1}{2} a K_t [A(t)] \{\Delta(t)\}, \quad (7)$$

As mentioned in previous section, $[A(t)]$ is periodic at the tooth passing frequency $\omega = N\Omega$, therefore its Fourier series expansion is used for the solution of the system. The average value in the Fourier series expansion (single frequency solution) of the time varying directional coefficients is used in this paper. Hence, (7) reduces to

$$\{F(t)\} = \frac{1}{2} a K_t [A_0] \{\Delta(t)\}, \quad (8)$$

where $[A_0]$ is the time invariant, but immersion dependent directional cutting coefficient matrix.

From the frequency response function FRF and the dynamic forces, the dynamic displacement vector in (8) can be solved. Using the response at present time $(t)$ and the previous tooth period $(T-t)$, equation (8) can be expressed as [14, 22]

$$\{F\} e^{i\omega_c t} = \frac{1}{2} a K_t [A_0] \left(1 - e^{-i\omega_c T}\right) [G(i\omega_c)] \{F\} e^{i\omega_c t}, \quad (9)$$

where $\{F\}$ represents the amplitude of the dynamic cutting force $\{F(t)\}$, $[G(i\omega_c)]$ is the transfer function matrix.

The transfer function matrix $[G(i\omega_c)]$ is the main focus of this paper. It is defined as

$$[G(i\omega_c)] = [G_c(i\omega_c)] + [G_w(i\omega_c)], \quad (10)$$

where

$$[G_p(i\omega_c)] = \begin{bmatrix} G_{p_{xx}}(i\omega_c) & G_{p_{xy}}(i\omega_c) \\ G_{p_{yx}}(i\omega_c) & G_{p_{yy}}(i\omega_c) \end{bmatrix}, \quad (p = c, w) \quad (11)$$

Equation (9) has a non-trivial solution only if its determinant is zero,

$$\det[[I] + \Lambda[G_0(i\omega_c)]] = 0, \quad (12)$$

where $[G_0] = [A_0][G]$

The eigenvalues is defined as

$$\Lambda = -\frac{N}{4\pi} K_t a \left(1 - e^{-i\omega T}\right), \quad (13)$$

Solving (12) numerically will give eigenvalues with complex and real parts $\left(\Lambda = \Lambda_R + i\Lambda_I\right)$, and from Euler's formula, $e^{-i\omega_c T} = \cos\omega_c T - i\sin\omega_c T$. When this is substituted into (13), the complex part has to vanish (i.e. $\Lambda_I(1 - \cos\omega_c T) = \Lambda_R \sin\omega_c T$) because the axial depth

of cut $a$ is a real value. Therefore,

$$\kappa = \frac{\Lambda_I}{\Lambda_R} = \frac{\sin \omega_c T}{1-\cos \omega_c T} = \tan \psi, \tag{14}$$

where $\psi$ is the phase shift of the eigenvalues. From this expression the relationship between the frequency and the spindle speed is [15] obtained

$$\begin{aligned} &\omega_c T = \varepsilon + 2k\pi, \\ &\varepsilon = \pi - 2\psi, \\ &\psi = \tan^{-1} \kappa, \\ &n = \frac{60}{NT}, \end{aligned} \tag{15}$$

where $\varepsilon$ is the phase difference between the inner and outer undulations, $k$ is an integer corresponding to the number of vibration waves within a tooth period and $n$ is the spindle speed (rpm). Substituting (14) into (13) and the final expression for chatter free axial depth of cut becomes

$$a_{\lim} = -\frac{2\pi\Lambda_R}{NK_t}\left(1+\kappa^2\right) \tag{16}$$

Therefore for a given chatter frequency, $\omega_c$ the eigenvalues are obtained from (12), which allows for the critical depth of cut to be calculated using (16) and finally the spindle speed using (15) for different number of vibration waves, $k$. This is repeated for various frequencies around the structures dominant modes.

The System's Transfer Function

To obtain the transfer function of the system, the modal dynamic analysis on Abaqus was used. Being a very well developed model, the modal dynamic analysis gives the response of a defined domain as a function of time for a given time dependent loading. This gives the linear response of the structure, which can be very easily extracted once the modes of the system are available. This is due to the modes being orthogonal, thereby rendering the system as a mere combination of single degree of freedom systems. The modes are extracted in a frequency extraction analysis, which utilizes the Lanczos algorithm. The free vibration solution of the equation of motion takes the form

$$\{x\} = \{X\}\sin \omega t \tag{17}$$

When substituted into equation of motion, an eigenvalue problem is obtained as

$$\left(\left[K\right] - \omega^2 \left[M\right]\right)\{X\} = 0, \tag{18}$$

where $\left[K\right]$ is the stiffness matrix of the system, $\left[M\right]$ is the mass matrix, $\omega_n^2$ is the eigenvalue or in this case the undamped natural frequency of the system squared and $\{X\}$ is the eigenvector (the mode of vibration or mode shape).

Being a large eigenvalue problem, the eigenvalues are extracted using the Lanczos method. The algorithm is detailed by Grimes et al. [24] and in Abaqus user manual [25].

Therefore, when the model is projected onto the eigenmodes (assuming the projected damping matrix is diagonal), the following expression at time $t$ is obtained [25]

$$\ddot{q}_r + 2\xi_r \omega_{n,r} q_r + \omega_{n,r}^2 q_r = f_{t-\Delta t} + \frac{\Delta f}{\Delta t}\Delta t, \tag{19}$$

where $r$ is the mode number, $q_r$ is the amplitude of the response of mode $r$ (in the ''generalized coordinate''), $\omega_{n,r}$ is the undamped natural frequency of mode $r$, $\Delta f$ is the change in $f$ over the time increment, $\Delta t$ assuming the excitation varies linearly within each increment and $\xi_r$ is the critical damping ratio for mode $r$ defined as

The solutions is simply obtained in the form

$$\begin{Bmatrix} q_{t+\Delta t} \\ \dot{q}_{t+\Delta t} \end{Bmatrix} = \begin{bmatrix} d_{11} & d_{12} \\ d_{21} & d_{22} \end{bmatrix} \begin{Bmatrix} q_t \\ \dot{q}_t \end{Bmatrix} + \begin{bmatrix} e_{11} & e_{12} \\ e_{21} & e_{22} \end{bmatrix} \begin{Bmatrix} f_t \\ f_{t+\Delta t} \end{Bmatrix}, \tag{20}$$

where $i, j = 1,2$, $d_{ij}$ and $e_{ij}$ are constants, which are dependent on the three different cases of non-rigid body motion. These cases are based on the oscillation modes - underdamped, critical damping and overdamped. These constants are detailed in Abaqus user manual [25].

Since the time integrations is done in generalized coordinates, the response of the physical variables are obtained through summation

$$u = \sum_r X_r q_r, \tag{21}$$

where $X_r$ are the eigenvector corresponding to the mode $r$ and $u$ is the actual nodal displacement. From this the velocity and hence the nodal acceleration can be derived.

The system's frequency response function (FRF), is simply the ratio of the Fourier transform of the output over the input (in the case of a system with single input and output).

$$G_{p_{nn}}(\omega) = \frac{X_{p_{nn}}(\omega)}{F_{p_{nn}}(\omega)} \quad (p = c, w), (n = x, y) \tag{22}$$

The discrete Fourier transform algorithm is adopted, which is defined [26] as

$$\begin{aligned} \operatorname{Re} H[k] &= \sum_{i=0}^{M-1} h[i] \cos\left(\frac{2\pi k t}{M}\right), \\ \operatorname{Im} H[k] &= -\sum_{i=0}^{M-1} h[i] \sin\left(\frac{2\pi k t}{M}\right), \end{aligned} \tag{23}$$

where $k$ runs from $0$ to $M/2$, $\operatorname{Re} H[k]$ and $\operatorname{Im} H[k]$ are the real and imaginary parts of the frequency domain signal and $h[i]$ is the time domain signal.

The corresponding frequencies are defined as

$$\omega = \frac{k \cdot f}{M-1}, \tag{24}$$

were $\omega$ is the frequency, $f$ is the sampling frequency.

## III. The Finite Element Model

The workpiece material used in the FEM model is Aluminium Alloy 7010 T7651. The material properties required for generating the stiffness and mass matrices are: Density - $2.823 \times 10^3$ Kg m$^{-3}$, Young's Modulus - 69.809 GPa and Poisson Ratio - 0.337. Three different types of

workpiece were used in the finite element analysis (FEA). The dimensions are shown in Figure 2 and the different thicknesses, ($W$) are shown in tables 1, 2 and 3 respectively.

The assumptions made in the finite element analysis (FEA) are as follows:

1) The workpiece was bolted at the back surface during the impact tests and in the FEM this was assumed to be clamped.
2) The workpiece was bolted to the milling machine during the impact test and it was assumed that the natural frequencies of the machine are very high compared to that of the workpiece, hence their influence can be ignored in the FEM analysis.
3) The mass of the accelerometer was assumed to be a point mass added to the FEM model.

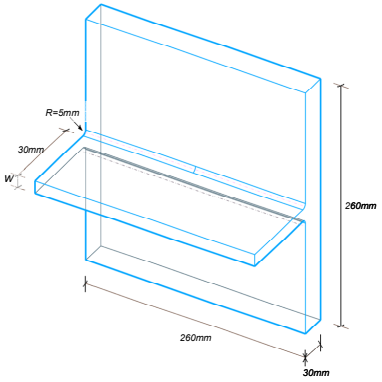


Fig. 2 – Workpiece dimensions.

Table 1 – Workpiece A, *W = 1.5mm*

| Mode Number | Natural Frequency, $\omega_n$ (Hz) | Damping Ratio, $\xi$ (%) |
|---|---|---|
| 1 | 1323.00 | 2.9345E-02 |
| 2 | 1604.00 | 2.6765E-03 |
| 3 | 1708.00 | 1.9422E-03 |
| 4 | 1908.00 | 2.2348E-03 |
| 5 | 2196.00 | 1.4750E-03 |
| 6 | 2566.00 | 1.6500E-03 |
| 7 | 3021.00 | 2.0739E-03 |
| 8 | 3571.215 | 8.0504E-03 |

Table 2 – Workpiece B, *W = 3.0mm*

| Mode Number | Natural Frequency, $\omega_n$ (Hz) | Damping Ratio, $\xi$ (%) |
|---|---|---|
| 1 | 2830.5000 | 2.5449E-02 |
| 2 | 3204.5000 | 4.4995E-03 |
| 3 | 3406.0000 | 2.9076E-03 |
| 4 | 3798.0000 | 4.8137E-03 |
| 5 | 4372.0000 | 5.3524E-03 |

Table 3 – Workpiece C, *W = 4.5mm*

| Mode Number, | Natural Frequency, $\omega_n$ (Hz) | Damping Ratio, $\xi$ (%) |
|---|---|---|
| 1 | 4253.0000 | 3.4222E-02 |
| 2 | 4568.0000 | 9.0496E-03 |
| 3 | 4894.0000 | 8.2851E-03 |

The Damping Ratio

The damping ratios, $\xi_r$ used in (19) were identified through impact tests and are given in tables 1, 2 and 3. The workpiece is excited using an instrumented hammer, whilst the accelerometer is placed on the opposite side of the impact point, to measure the direct transfer function. Using a Fourier analyser, the accelerance frequency response function is extracted for each impact test. This is simply the division of the Fourier transform of the measured time domain input force $f(t)$ and acceleration $\ddot{x}(t)$.

$$Acc(\omega) = \frac{\ddot{X}(\omega)}{F(\omega)}, \tag{25}$$

where $Acc(\omega)$ is the accelerance FRF, $\ddot{X}(\omega)$ is the output acceleration signal in frequency domain and $F(\omega)$ is the input force signal in frequency domain. The experimental measurements are analysed using a modal analysis system (CutPro was used for the solutions in this paper), which scans the measured transfer function and fits a curve to the data in order to obtain the numerical values of natural frequency, damping [27].

## IV. Results

### A. Extracting the Workpiece Transfer Function.

For workpiece A, the measured input force from the impact test was used as the input force (in time domain) in the FEM modal analysis. The predicted acceleration (time domain) is shown in comparison to the experimental acceleration from the accelerometer (during the impact test) in Figure 3. The predicted FRF (using the approach in section 2) and experimental FRF, are compared in Figures 4 a and b respectively. The agreement between the experimental results and the predictions is satisfactory.

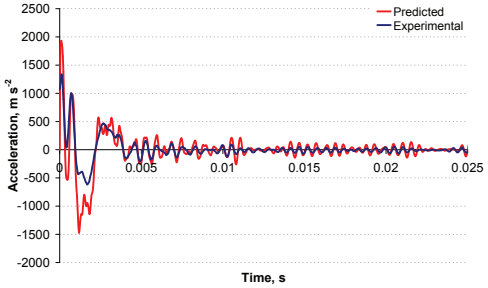


Fig. 3 – Predicted and measured acceleration for workpiece A.

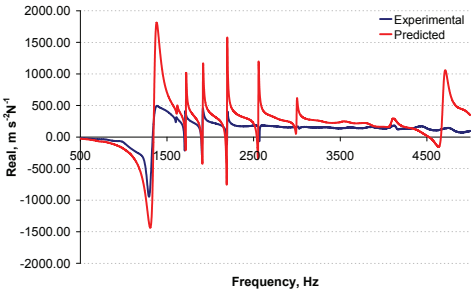


(a) Real

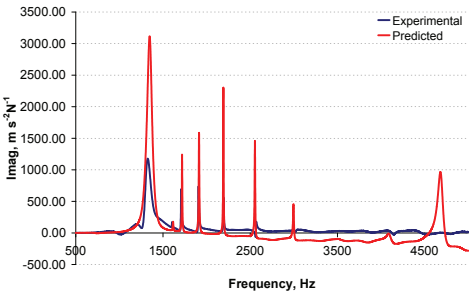


(b) Imag

Fig. 4 – Predicted and measured FRFs for workpiece A, $G_{w_{yy}}$.

For workpiece B, the input force (in time domain) used in the FEM modal analysis was a Dirac delta function. The predicted and experimental FRFs are compared in Figures 5. The agreement between the experimental results and the predictions is satisfactory.

Figure 6 compares the predicted and experimental FRFs for workpiece C and the agreement has shown to be good.

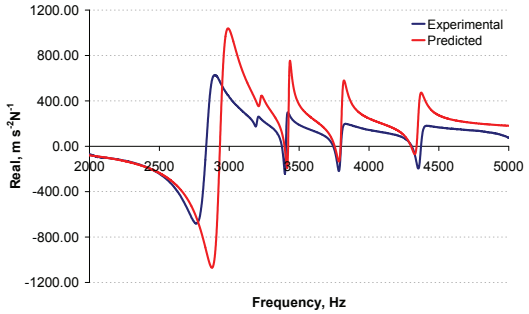


(a) Real

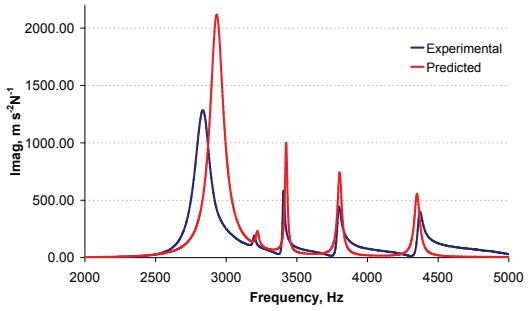


(b) Imag

Fig. 5 – Predicted and measured FRFs for workpiece B, $G_{w_{yy}}$ .

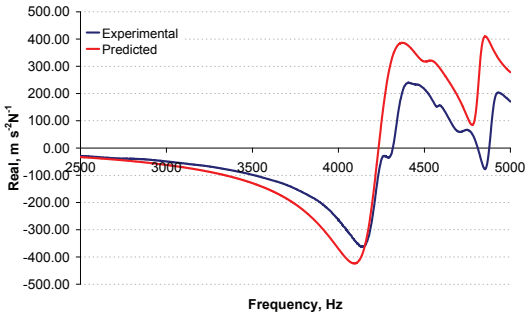


(a) Real

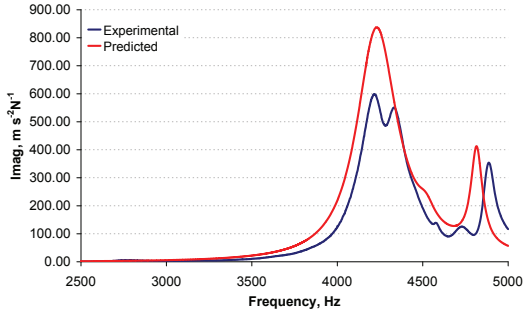


(b) Imag

Fig. 6 – Predicted and measured FRFs for workpiece C, $G_{w_{yy}}$ .

### *B. Chatter Stability Lobes.*

Using both the predicted and experimental FRFs, the stability lobes was generated using CutPro, for the different types of workpiece using the parameters listed in table 4. CutPro is an analytical and time-domain machining process simulation commercial package developed by Altintas. It has an in built modal analysis module and also a stability lobes module. The stability lobes module can take the transfer function in all three orthogonal directions for the workpiece and transfer function in x, and y directions for the tool. The predicted and experimental results are compared in Figures. 7a, b & c for the three different workpiece. The comparisons show a satisfactory agreement. The slight discrepancy in the predicted natural frequency (frequency at which FRF real is zero and imaginary is maximum) can be seen in the slight shift in the spindle speed calculated in the stability lobes. The natural frequency predicted affects the stable tooth passing frequency calculated in the stability lobes, hence the slight differences seen in the spindle speeds.

Table 4

| | WORKPIECE A | WORKPIECE B | WORKPIECE C |
|---|---|---|---|
| RCFC, $K_r$ | -0.7040 | 0.3030 | 1.1459 |
| TCFC, $K_t$ (MPa) | 981.6966 | 801.0970 | 679.6021 |
| Radial depth of Cut, (mm) | 0.500 | 1.000 | 2.000 |

where "RCFC" is the radial cutting force coefficient and "TCFC" is the tangential cutting force coefficient.

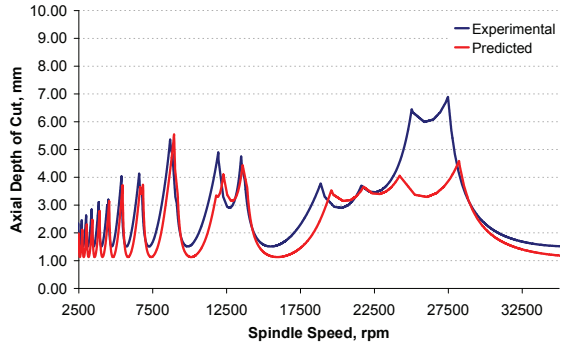


(a) Workpiece A

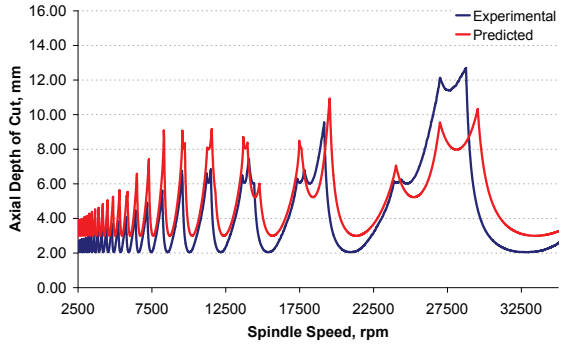


(b) Workpiece B

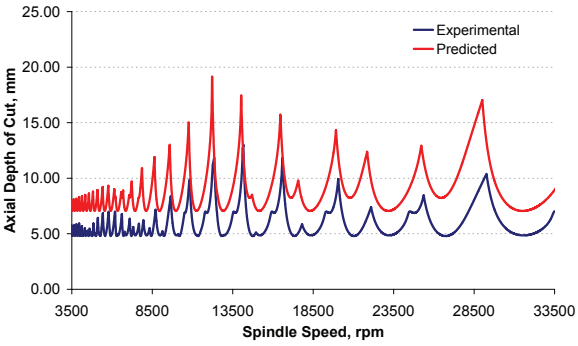


(b) Workpiece C

Fig. 7 – Stability lobes comparison.

The predicted stable axial depth of cuts in Figures 7 b and c are slightly higher than the experimental stable ADOC and this is due to the FEM model being too stiff. This can be caused by the boundary condition assumption stated in section 3, where the back surface was assumed to be perfectly clamped. In the FEM stiffness matrix formulation, the elements are therefore set to 1E+36 and the degrees of freedom at this surface are not included in the simulation. A more accurate approach would require knowledge of the friction at the boundary between the machine and the workpiece.

For completeness, the full FRF matrix in (11) is required, however applying the impact force and/or measuring the response in certain directions experimentally can prove difficult. Using the proposed approach however, the full FRF matrix in (11) can be obtained easily in all directions. This is done by simply applying the impact force in the corresponding directions of interest.

## V. Conclusion

Chatter still undermines the efforts of the machinist by reducing surface quality, productivity and increasing cost in damage repair. In this paper, an alternative approach to extracting the transfer function using the FEM modal analysis has been presented. The approach is based on the Fourier transform of the results obtained from the finite element analysis. The results are shown to agree with experimental results and hence the transfer function calculated. Its accuracy is further explored by its use in stability lobe predictions. This approach can be used to solve different problems encountered through the use of impact test, including obtaining the frequency response function in directions that ca prove difficult experimentally.

## Acknowledgements

The authors acknowledge the support given by EPSRC for funding this project and also the immense support given by Airbus along with Mr Alister (GKN Aerospace).

## Reference

[1] F. W. Taylor, On the art of cutting metals, *Transactions of the American Society of Mechanical Engineers,* 28, 1907, pp. 31–350.
[2] S. A. Tobias and W. Fishwick, A Theory of Regenerative Chatter, The Engineer London (1958).
[3] J. Tlusty and M. Polacek, The Stability of Machine Tools Against Self Excited Vibrations in Machining, International Research in Production Engineering ASME, (1963), pp. 465 – 474.
[4] H. E. Merritt, Theory of Self-Excited Machine Tool Chatter, ASME Journal of Engineering for Industry, 87, (1965), pp. 447 – 454.
[5] R Sridhar, R. E. Hohn and G. W. Long, General Formulation of the Milling Process Equation, ASME Journal of Engineering for Industry, (1968), pp. 317 – 324.
[6] J. Slavicek, The Effect of Irregular Tooth Pitch on Stability of Milling, 6th MTDR Conference Manchester, (1965).
[7] P. Vanherck, Increasing Milling Machine Productivity by Use of Cutters with Non-Constant Cutting – Edge Pitch, 8th MTDR Conference Manchester, (1967).
[8] J. Tlusty and F. Koenigsberger, Machine Tool Structures, Pergamon Press Oxford 5th Edn., Vol. 1, (1970).
[9] H. Opitz, Chatter Behaviour of Heavy Machine Tools, Quarterly Technical Report No. 2 AF 61 (052) – 916 Research and Technology Division Wright Patterson Air Force Base OH., (1968).
[10] H. Opitz and F. Bernardi, Investigation and Calculation of the Chatter Behaviour of Lathes and Milling Machines, Annals of the CIRP, 18, (1970), pp. 335 – 343.
[11] I. Minis and T. Yanushevsky, A New Theoretical Approach for the Prediction of Machine Tool Chatter in Milling, ASME Journal of Engineering for Industry, 115, (1993), pp. 1-8.
[12] I. Minis and T. Yanushevsky, R. Tembo and R. Hocken, Analysis of Linear and Nonlinear Chatter in Milling, Annals of the CIRP, 39, (1990), pp. 459 – 462.
[13] A. C. Lee and C. S. Liu, Analysis of Chatter Vibration in the End Milling Process, International Journal of Machine Tool Design and Research, 31(4), (1991), pp. 471 – 479.
[14] A. C. Lee, C. S. Liu and S. T. Chiang, Analysis of Chatter Vibration in a Cutter – Workpiece System, International Journal of Machine Tool Design and Research, 31(2), (1991), pp. 221 – 234.
[15] Y. Altintas and E. Budak, Analytical Prediction of Stability Lobes in Milling, Annals of the CIRP, 44(1), (1995), pp. 357 – 362.
[16] S. D. Merdol and Y. Altintas, Multi Frequency Solution of Chatter Stability for Low Immersion Milling, Journal of Manufacturing Science and Engineering, Transactions of the ASME, 126(3), (2004), pp. 459 – 466.
[17] U. Bravo, O. Altuzarra, L. N. Lopez de Lacalle, J. A. Sanchez, F. J. Campa, Stability limits of milling considering the flexibility of the workpiece and the machine, International Journal of Machine Tools and Manufacture, 45(15), (2005), pp. 1669 – 1680.
[18] E. Solis, C. R. Peres, J. E. Jimenez, J. R. Alique, J. C. Monje, A new analytical–experimental method for the identification of stability lobes in high-speed milling, International Journal of Machine Tools and Manufacture, 44(15), (2004), pp. 1591 – 1597.
[19] H. B. Lacerda, V. T. Lima, Evaluation of Cutting Forces and Prediction of Chatter Vibrations in Milling, Journal of the Brazilian Society of Mechanical Sciences and Engineering, 26(1), (2004), pp. 74 – 81.
[20] E. Budak and Y. Altintas, Analytical Prediction of Chatter Stability in Milling – Part I: General Formulation, Transactions of the ASME, 120, (1998), pp. 22 – 30.
[21] E. Budak and Y. Altintas, Analytical Prediction of Chatter Stability in Milling – Part II: Application of the General Formulation to Common Milling Systems, Transactions of the ASME, 120, (1998), pp. 31 – 36.
[22] E. Budak, Mechanics and Dynamics of Milling Thin Walled Structures, PhD thesis, The University of British Columbia, (1994).
[23] E. Budak, Analytical models for high performance milling. Part II: Process dynamics and stability, International Journal of Machine Tools & Manufacture, 46, (2006), pp. 1489 – 1499.
[24] R. G. Grimes, J. G. Lewis and H. D. Simon, A Shifted Block Lanczos Algorithm for Solving Sparse Symmetric Generalized Eigenproblems, SIAM Journal on Matrix Analysis and Applications, 15, (1994), pp. 228 – 272.
[25] Karlsson & Sorensen, Inc. Hibbitt, Abaqus Theory Manual, 1080 Main Street Pawtucket Rl 02860 – 4847 USA, (2006).
[26] S. W. Smith, The Scientist & Engineer's Guide to Digital Signal Processing, California Technical Pub. San Diego, 1st edition, (1997). Available: http://www.dspguide.com
[27] Y. Altintas, Manufacturing Automation, Cambridge University Press, New York, NY (2000).